PHYSICAL REVIEW D **95,** 124033 (2017)

Collapse and bounce of null fluids

Bradley Creelman[*] and Ivan Booth[†]

Department of Mathematics and Statistics, Memorial University of Newfoundland, St. John's, Newfoundland and Labrador A1C 5S7, Canada

(Received 9 November 2016; published 21 June 2017)

Exact solutions describing the spherical collapse of null fluids can contain regions which violate the energy conditions. Physically the violations occur when the infalling matter continues to move inward even when nongravitational repulsive forces become stronger than gravity. In 1991 Ori proposed a resolution for these violations: spacetime surgery should be used to replace the energy condition violating region with an outgoing solution. The matter bounces. We revisit and implement this proposal for the more general Husain null fluids including a careful study of potential discontinuities and associated matter shells between the regions. Along the way we highlight an error in the standard classification of energy condition violations for type II stress-energy tensors.

DOI: 10.1103/PhysRevD.95.124033

I. INTRODUCTION

Vaidya spacetimes are the best known exact solutions describing dynamical black (or white) holes. The basic solution describes a null dust infalling onto a black hole (or radiating from a white hole) and was later generalized to charged null dust in [1] and to a null fluid with pressure in [2]. Focusing on collapse solutions, the inclusion of these extra interactions can result in regions where the energy conditions are violated (see, for example, [2–5]). For collapsing matter, these are regions where the fluid continues moving inward despite nongravitational repulsive forces becoming stronger than the gravitational attraction [Fig. 1(a)].

For the case of the charged Vaidya solution, Ori [3] argued for a construction to remove the apparent violations. By carefully considering the Lorentz force on the dust and thus including a Lorentz force term in the equations of motion, he showed that on the hypersurface dividing regular spacetime from the region of violations, the wave vector of the fluid vanishes.

This suggested a physical reinterpretation of charged Vaidya in which the vanishing wave-vector hypersurface signals a bounce from infalling to outgoing dust. Geometrically this reinterpretation corresponds to a new hybrid spacetime built from violation-free regions of infalling and outgoing Vaidya solutions (Fig. 1). These regions join along a common spacelike bounce surface.[1]

This bounce resolves the energy condition violations with the critical hypersurface corresponding physically to the location where the Lorentz repulsive force overcomes gravity and the charged fluid turns around. This interpretation is consistent with the null limit for timelike fluids [3] as well as the evolution of null charged particles in Reissner-Nordström (RN) spacetimes [3] (and Appendix A of this paper) and null charged thin shells [8].

Generalizations of this procedure have recently been applied to modified $f(R)$ theories of gravity [9] as well as the extremal case of the charged Vaidya solution [10]. However in [10] a possible inconsistency was noted in Ori's original calculation. In [3] it was found that the extrinsic curvatures of the component spacetimes matched along the junction and so, by the standard Israel-Darmois junction conditions [11], the connection is smooth to first order. In [10] it was shown that, at least in the extremal case, the extrinsic curvatures do not match and so a thin-shell discontinuity (which is the instantaneous appearance of a stress tensor) is required to connect the spacetimes across the bounce surface. Though this was a very special limiting case, it was in tension with the apparently more general result.

In this paper we revisit Ori's construction with two goals. First, we generalize to Husain null fluid spacetimes [2]. In general these are interpreted as null fluids with pressure, however they include Vaidya Reissner-Nordström (VRN) as a special case where the energy density and pressure are reinterpreted as arising from a Maxwell field. Second, we carefully reexamine the spacetime surgery to determine whether or not there is a thin-shell discontinuity. When looking at the more general case of Husain null fluids, we also answer the question as to why there are conflicting results in [3,10]: it turns out that both are mathematically correct but differ due to a choice in how to match along the junction hypersurface.

In general, when matching two spacetimes along a spacelike hypersurface, there will not be a unique way in which the matching can take place. We find that in

[*]bjc527@mun.ca
[†]ibooth@mun.ca

[1]This is not a physical restriction but rather based on the available solutions. A timelike bounce would necessarily include regions with both infalling and outgoing dust but we do not have an exact solution describing this situation. Hence the construction can only be used to describe spacelike bounces.

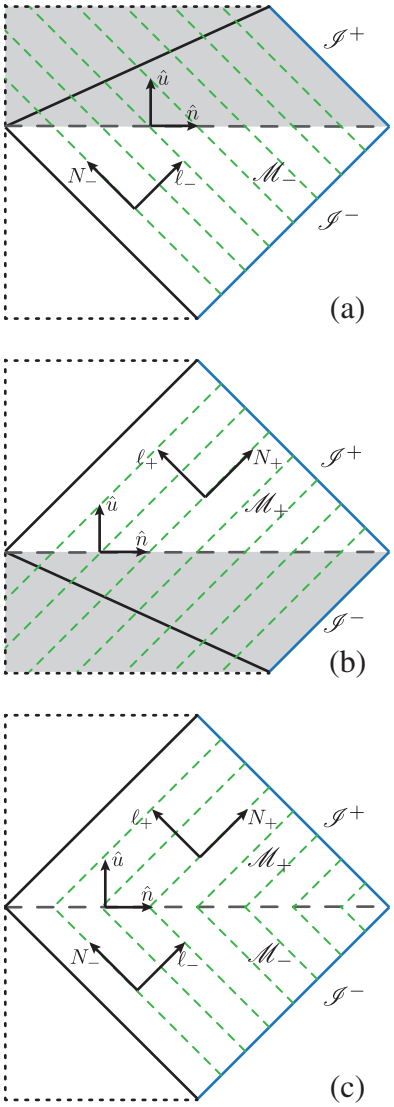

FIG. 1. Surgery to remove energy condition violating regions from Vaidya Reissner-Nordström. (a) shows infalling Vaidya RN (dust accreting onto a RN black hole) while (b) shows outgoing Vaidya RN (dust being emitted from a RN white hole). In both cases energy condition violations exist in the shaded region. However, as shown in (c) if energy condition violating regions of each spacetime are removed along the spacelike dashed line, then the remaining pieces may be reconnected into a nonenergy condition violating spacetime (apart from maybe at the junction—see Sec. III). In all diagrams, apparent rather than event horizons are shown and so in regions where matter crosses the horizon they are spacelike (see, for example, [6,7]). The dotted lines on all figures indicate that they continue in those directions (but into regions that are not of direct interest for us). Note that in the violation-free spacetimes, matter crosses neither the black hole nor the white hole horizon.

general there are two distinct ways to match the spacetimes along the bounce surface: a time reflection and a second, more complicated, matching (which in the static case is simply equivalent to the transformation from ingoing to outgoing coordinates). For extremal VRN, only the time reflection is possible and in that case it is intuitively clear that the extrinsic curvatures will be the negatives of each other. However this does not show that there is also a thin shell in Ori's case: he used the second matching. In that case the shell vanishes not only for VRN but also for the more general Husain null fluids. Thus the two results do not contradict each other.

Along the way we note another, minor result. Almost all stress-energy tensors studied in this paper are of type II [12]. Since we are concerned with energy condition violations, we reexamined those conditions and were surprised to find an error in their original presentation in [12]. While we have subsequently learned that this has been previously noted (see, for example, [13–16]), the error is not universally known and the incorrect conditions have been and continue to be used in the literature (see, for example, [2,9,17–21]). As such for future reference we explicitly present the correct form of the energy conditions in an Appendix B to this paper.

The paper is organized as follows. Section II reviews Husain null fluids as a generalization of the charged Vaidya solution and discusses energy condition violations in these spacetimes. Section III considers the (non)existence of a thin shell at a spacelike junction hypersurface for the Husain spacetimes and examines other possible discontinuities in the matter fields. Section IV demonstrates a concrete example of the matching conditions and so confirms that the conditions assumed in the previous section are consistent with real examples. Section V reviews and discusses implications of the work. Finally, Appendix A reviews null particle paths in Reissner-Nordström spacetimes while Appendix B studies the energy conditions for type II stress-energy tensors.

For notation, early alphabet latin letters $(a, b, c, \ldots)$ are used as four-dimensional abstract indices, greek letters $(\alpha, \beta, \gamma, \ldots)$ are used as four-dimensional coordinate indices and midalphabet latin letters with hats $(\hat{\imath}, \hat{\jmath}, \hat{k}, \ldots)$ are used as indices for a three-dimensional orthonormal spacelike triad spanning the tangent space of the junction surface.

II. HUSAIN NULL FLUIDS

In this section, we review the geometry and physics of the Husain null fluid spacetimes as presented in [2] and the occurrence of energy condition violations for these solutions.

A. The spacetime

The (infalling) Husain solution is obtained by assuming a general spherically symmetric solution with mass function $m(v, r)$:

$$ds^2 = -\left(1 - \frac{2m(v,r)}{r}\right)dv^2 + 2dvdr + r^2 d\Omega^2, \quad (1)$$

where v labels infalling null geodesics and r (the areal radius) is an affine parameter along those geodesics: see Fig. 1(a).

Then from the Einstein equations, the associated stress-energy tensor may be written relative to radially outward- and inward-pointing null vectors,

$$\ell = \frac{\partial}{\partial v} + \frac{1}{2}\left(1 - \frac{2m(v,r)}{r}\right)\frac{\partial}{\partial r} \tag{2}$$

and

$$N = -\frac{\partial}{\partial r}, \tag{3}$$

as

$$T_{ab} = \mu N_a N_b - \rho q^{\perp}_{ab} + P\tilde{q}_{ab}, \tag{4}$$

where $\tilde{q}_{ab}$ and $q^{\perp}_{ab}$ are respectively the induced metric on the surfaces of constant (v,r) and that on the normal space to those surfaces:

$$q^{\perp}_{ab} = -\ell_a N_b - N_a \ell_b \tag{5}$$

and

$$\tilde{q}_{ab} = g_{ab} - q^{\perp}_{ab}. \tag{6}$$

Further,

$$\mu = \frac{m_v}{4\pi r^2}, \tag{7}$$

$$\rho = \frac{m_r}{4\pi r^2}, \tag{8}$$

and

$$P = -\frac{m_{rr}}{8\pi r}. \tag{9}$$

where the subscripts are partial derivatives.

Interpreting these components of the stress-energy tensor, this is an inward falling, self-interacting null fluid. μ is the flux of energy in the (inward) N^α direction, while ρ is the energy density associated with the self-interaction and P is a tangential pressure.

At this stage $m(v,r)$ is arbitrary, however restrictions on its allowed forms are imposed by the energy conditions as outlined in Appendix B. For individual energy conditions, the restrictions that we find are not equivalent to those given in [12], however the restrictions imposed if we require that all four energy conditions hold are equivalent. Requiring that the weak, null, dominant and strong all hold for (4), we must have

$$\mu \geq 0, \qquad \rho \geq 0, \quad \text{and} \quad 0 \leq P \leq \rho. \tag{10}$$

That is,

$$m_v \geq 0, \qquad m_r \geq 0, \quad \text{and} \quad -2m_r \leq r m_{rr} \leq 0. \tag{11}$$

B. Polytropic fluids

1. (a = 1) fluid infalling onto a black hole

Even with the energy condition restrictions the range of allowed forms for $m(v,r)$ is still large. However for any particular null fluid one expects an equation of state to relate at least the pressure P and energy density ρ. Husain focuses on polytropic fluids for which

$$P = k\rho^a, \tag{12}$$

for some constants k and a. For our purposes it will be sufficient to consider fluids for which $a = 1$. Other, more complicated equations of state are considered in [2].

$P = k\rho$ yields an integrable equation for the mass function $m(v,r)$ and has the solution

$$m(v,r) = M(v) - \frac{g(v)}{2r^{2k-1}}, \tag{13}$$

where $M(v)$ and $g(v)$ are arbitrary functions. That is,

$$ds^2 = -\left(1 - \frac{2M(v)}{r} + \frac{g(v)}{r^{2k}}\right)dv^2 + 2dvdr + r^2 d\Omega^2. \tag{14}$$

We restrict our attention to asymptotically flat spacetimes $k > \frac{1}{2}$. Note in particular that choosing $k = 1$ and $g(v) = Q(v)^2$ we recover the charged Vaidya solution.

2. Energy conditions

Let us now consider restrictions imposed on these solutions by the energy conditions. First for (14)

$$\rho = \frac{m_r}{4\pi r^2} = \frac{(2k-1)}{8\pi}\frac{g(v)}{r^{2k+2}}. \tag{15}$$

Hence with $k > \frac{1}{2}$,

$$\rho \geq 0 \Rightarrow g(v) \geq 0 \tag{16}$$

and so we can rewrite the line element of the Husain spacetime as

$$ds^2 = -\left(1 - \frac{2M(v)}{r} + \left(\frac{\Xi(v)}{r}\right)^{2k}\right)dv^2 + 2dvdr + r^2 d\Omega^2, \tag{17}$$

where we have rewritten $g(v) = \Xi(v)^{2k}$ so that the free function $\Xi(v)$ will have dimensions of length. For $k = 1$ we recover VRN with $\Xi(v) = Q(v)$.

Next

$$0 \leq P \leq \rho \Rightarrow k \leq 1 \tag{18}$$

and so now k is bound both above and below: $\frac{1}{2} < k \leq 1$.

Finally $\mu \geq 0$ requires

$$m_v = M_v - k\Xi_v \left(\frac{\Xi}{r}\right)^{2k-1} \geq 0. \tag{19}$$

Unlike other violations this one cannot always be removed by restricting our attention to a subclass of solutions. Defining

$$R_o = \Xi\left(k\left|\frac{\Xi_v}{M_v}\right|\right)^{1/(2k-1)}, \tag{20}$$

there are four cases:

(1) $\Xi_v > 0$, $M_v \leq 0 \Rightarrow$ violations for all r,
(2) $\Xi_v > 0$, $M_v > 0 \Rightarrow$ violations for $r < R_o$,
(3) $\Xi_v < 0$, $M_v < 0 \Rightarrow$ violations for $r > R_o$,
(4) $\Xi_v < 0$, $M_v \geq 0 \Rightarrow$ no violations.

As a special case note that if $\Xi_v \Xi^{2k-1} = 0$ then there are no violations as long as $M_v \geq 0$. These are VRN spacetimes but with uncharged dust.

For general VRN ($k = 1, \Xi = Q$) there are clear physical interpretations in analogy with the paths of null particles moving in a background RN field. Those paths are considered in some detail in Appendix A and in making the connection note that the radial evolution of any particular shell of constant v is equivalent to that of a corresponding particle of with an energy at infinity of

$$E_\infty = \frac{M_v}{4\pi} \tag{21}$$

and charge

$$q = \frac{Q_v}{4\pi r^2} \tag{22}$$

moving in a background RN spacetime with $Q = Q(v)$ and $M = M(v)$. Then the four cases above respectively map onto cases I_{+-}, I_{++}, I_{--}, and I_{-+} from Appendix A.

The interpretation of M_v as proportional to energy at infinity continues for the $k \neq 1$ cases however the individual particle interpretation is then not so clear.

3. (a = 1) fluid radiating from a white hole

Thus far we have considered spacetime with matter infalling onto a black hole, however a judicious application of negative signs switches these solutions to ones with matter radiating from a white hole.

In this case the line element is

$$ds^2 = -\left(1 - \frac{2M(u)}{r} + \left(\frac{\Xi(u)}{r}\right)^{2k}\right)du^2 - 2dudr + r^2 d\Omega^2, \tag{23}$$

where u labels the outgoing radial null geodesics and r is still the affine parameter. The stress-energy tensor still takes the form (4) though this time for null vectors:

$$\ell = \frac{\partial}{\partial v} - \frac{1}{2}\left(1 - \frac{2m}{r}\right)\frac{\partial}{\partial r}, \tag{24}$$

$$N = \frac{\partial}{\partial r}. \tag{25}$$

N continues to point in the direction of the fluid motion and so in this case outward rather than inward.

The $\rho \geq 0$ and $0 \leq \rho \leq P$ conditions are unchanged and for $\mu \geq 0$ with

$$\tilde{R}_o = \Xi\left(k\left|\frac{\Xi_u}{M_u}\right|\right)^{1/(2k-1)}, \tag{26}$$

there are the same four cases:

(1) $\Xi_u > 0$, $M_u \leq 0 \Rightarrow$ violations for all r,
(2) $\Xi_u > 0$, $M_u > 0 \Rightarrow$ violations for $r < \tilde{R}_o$,
(3) $\Xi_u < 0$, $M_u < 0 \Rightarrow$ violations for $r > \tilde{R}_o$,
(4) $\Xi_u < 0$, $M_u \geq 0 \Rightarrow$ no violations.

Again the $k = 1$ the cases may be understood in terms of the evolution of charged null particles in a RN background. This time they are the outgoing particles O_{+-}, O_{++}, O_{--}, and O_{-+} discussed in Appendix A.

III. SURGERY TO REMOVE ENERGY CONDITION VIOLATIONS

The complementary energy condition violations for infalling and radiating null fluids suggest replicating Ori's construction for these more general spacetimes. That is, for $M_v > 0$ excise the $r < R_o(v)$ section of an infalling spacetime (14) and replace it with the $r < \tilde{R}_o(u)$ section of a radiating spacetime (23) with the parameters chosen so that the induced metrics match on $r = R_o(v) = \tilde{R}_o(u(v))$ for some function $u(v)$.

As we shall now see, the Israel-Darmois junction conditions require $\frac{du}{dv} < 0$ along the matching surface. Thus, referencing the lists in Secs. II B 2 and II B 3, these are case $2 \leftrightarrow 3$ matchings.

A. Hypersurface geometry

First, we study the intrinsic and extrinsic geometry of spherically symmetric hypersurfaces.

It will be convenient to consider both infalling and radiating spacetimes simultaneously and so we write

$$ds^2 = -f(w,r)dw^2 + 2\epsilon dw dr + r^2 d\Omega^2, \tag{27}$$

where $\epsilon = \pm 1$ with $w = v$ (ingoing) for $\epsilon = 1$ and $w = u$ (outgoing) for $\epsilon = -1$. We leave the metric function in the general form

$$f(w,r) = 1 - \frac{2m(w,r)}{r}. \tag{28}$$

For this discussion the more specialized form (17) is not required and in fact it is simpler to write our expressions in terms of $f(w,r)$ or $m(w,r)$.

Now consider a general spherically symmetric hypersurface B parametrized by $w = W(\lambda)$ and $r = R(\lambda)$. Then the induced metric on B is

$$d\Sigma^2 = (-f\dot{W}^2 + 2\epsilon \dot{W}\dot{R})d\lambda^2 + R^2 d\Omega^2, \tag{29}$$

with dots indicating derivatives with respect to λ. We restrict our attention to spacelike B and so the functions must satisfy

$$\dot{W}(-f\dot{W} + 2\epsilon\dot{R}) > 0. \tag{30}$$

Turning to the extrinsic geometry it is convenient to work with a hypersurface-adapted tetrad. The timelike unit normal pointing in the positive w direction is

$$\begin{aligned}\hat{u}^\alpha \partial_\alpha &\equiv \hat{e}^\alpha_{(0)}\partial_\alpha \\ &\equiv \frac{1}{\sqrt{2\epsilon R_w - f}}\left(\frac{\partial}{\partial w} + (\epsilon f - R_w)\frac{\partial}{\partial r}\right),\end{aligned} \tag{31}$$

and the spacelike unit tangent pointing in the positive r direction is

$$\hat{n}^\alpha \partial_\alpha \equiv \hat{e}^\alpha_{(1)}\partial_\alpha \equiv \frac{\epsilon}{\sqrt{2\epsilon R_w - f}}\left(\frac{\partial}{\partial w} + R_w \frac{\partial}{\partial r}\right). \tag{32}$$

In both cases $R_w \equiv \frac{\dot{R}}{\dot{W}} = \frac{dR}{dw}$ if we reparametrize B as $r = R(w)$. Finally the tangential unit vectors are

$$\begin{aligned}\hat{e}^\alpha_\theta \partial_\alpha &\equiv \hat{e}^\alpha_{(2)}\partial_\alpha \equiv \frac{1}{r}\frac{\partial}{\partial\theta}, \\ \hat{e}^\alpha_\phi \partial_\alpha &\equiv \hat{e}^\alpha_{(3)}\partial_\alpha \equiv \frac{1}{r\sin\theta}\frac{\partial}{\partial\phi}.\end{aligned} \tag{33}$$

The extrinsic curvature of B relative to the tetrad is

$$K_{ij} = \hat{e}^\alpha_i \hat{e}^\beta_j \nabla_\alpha \hat{u}_\beta. \tag{34}$$

That is,

$$\begin{aligned}K = &\left(\frac{-\epsilon(2R_{ww} + f f_r) + (f_w + 3f_r R_w)}{2(2\epsilon R_w - f)^{3/2}}\right)(\hat{n}\otimes\hat{n}) \\ &+ \left(\frac{\epsilon f - R_w}{r\sqrt{2\epsilon R_w - f}}\right)(\hat{e}_\theta\otimes\hat{e}_\theta + \hat{e}_\phi\otimes\hat{e}_\phi).\end{aligned} \tag{35}$$

Subscripts indicate (partial) derivatives: $f_r = \partial_r f$, $f_w = \partial_w f$, and $R_{ww} = \frac{d^2}{dw^2}R(w)$.

Finally note that relative to the hypersurface tetrad

$$\ell = \frac{\sqrt{2\epsilon R_w - f}}{2}(\hat{u} + \epsilon\hat{n}), \tag{36}$$

$$N = \frac{1}{\sqrt{2\epsilon R_w - f}}(\hat{u} - \epsilon\hat{n}). \tag{37}$$

The spacelike tangent vector n always points in the positive-r direction but ℓ and N are instead tied to the fluid flow and so change orientations depending on whether we are considering the infalling or radiating solution.

B. Matching infalling and radiation solutions across B: Geometry

Now consider B embedded into both an infalling spacetime $\mathcal{M}_-$ and a radiating spacetime $\mathcal{M}_+$ (the subscript indicates that in the final construction $\mathcal{M}_-$ will be in the past of $\mathcal{M}_+$ as in Fig. 1). Parametrize the two embeddings as

$$(v,r) = (V(\lambda), R(\lambda)) \quad \text{and} \quad (u,r) = (U(\lambda), \tilde{R}(\lambda)). \tag{38}$$

We then restrict our attention to matchings for which

$$f^-(U(\lambda), R(\lambda)) = f^+(V(\lambda), R(\lambda)). \tag{39}$$

While it may be possible to construct matchings for more general surfaces, this is both computationally convenient and gives rise to solutions with desirable physical properties (Sec. III C).

1. Matching the induced metric

Matching the components of the induced metrics (29) on B, the angular components give

$$R(\lambda) = \tilde{R}(\lambda) \tag{40}$$

and so henceforth we discard the tilde. The (λ,λ) components give

$$f\dot{V}^2 - 2\dot{V}\dot{R} = f\dot{U}^2 + 2\dot{U}\dot{R}, \tag{41}$$

where we have omitted the superscripts to distinguish the f's since they agree on B. Then the induced metrics match if

$$(\dot{V}+\dot{U})(f(\dot{V}-\dot{U})-2\dot{R})=0. \tag{42}$$

Thus there are two possible matchings[2] which we label as

$$\text{Reflective}:\ \dot{U}=-\dot{V}\Rightarrow U_v=-1 \quad \text{and} \tag{43}$$

$$\text{Ori}:\ \dot{U}=\dot{V}-\frac{2\dot{R}}{f}\Rightarrow U_v=1-\frac{2R_v}{f}, \tag{44}$$

where the right-hand expressions arise if we adopt the ingoing v as our surface parameter: $\lambda=v$. Henceforth we make this choice. Note that in both cases $U_v<0$.

As suggested by the label, the first solution (43) corresponds to a time-reversal symmetry between the regions: $K^+_{\hat{\imath}\hat{\jmath}}=-K^-_{\hat{\imath}\hat{\jmath}}$. This is the matching condition that was used in [10]. However the second solution (44) is the one that was used by Ori. For pure Schwarzschild or RN this is just the transformation that reparametrizes the surface from ingoing to outgoing coordinates.

Given that different matchings were being used the disagreement between the papers is not surprising. Note however that this was unavoidable, as in [10] the matching was along the apparent horizon where $f=0$ and so Ori's choice was not available (or noticed by the author).

2. Matter shell from matching the extrinsic curvatures

For either of these choices, we can apply the Israel-Darmois junction conditions [11] to calculate the stress tensor necessary to account for any discontinuities introduced by the construction. Recall that if the extrinsic curvatures of B in $\mathcal{M}_-$ and $\mathcal{M}_+$ are not equal then $K^-_{\hat{\imath}\hat{\jmath}}\neq K^+_{\hat{\imath}\hat{\jmath}}$ and there is a thin shell of matter at B with stress tensor

$$S_{\hat{\imath}\hat{\jmath}}=-\frac{1}{8\pi}([K_{\hat{\imath}\hat{\jmath}}]-[K]h_{\hat{\imath}\hat{\jmath}}), \tag{45}$$

where

$$[K_{\hat{\imath}\hat{\jmath}}]=K^+_{\hat{\imath}\hat{\jmath}}-K^-_{\hat{\imath}\hat{\jmath}} \tag{46}$$

and similarly $[K]=h^{\hat{\imath}\hat{\jmath}}[K_{\hat{\imath}\hat{\jmath}}]$. Then the radial and tangential pressure densities are respectively

$$S_{\hat{n}\hat{n}}=\frac{1}{4\pi}[K_{\hat{\theta}\hat{\theta}}], \tag{47}$$

$$S_{\hat{\theta}\hat{\theta}}=S_{\hat{\phi}\hat{\phi}}=\frac{1}{8\pi}([K_{\hat{\theta}\hat{\theta}}]+[K_{\hat{n}\hat{n}}]). \tag{48}$$

These components can be calculated from (35):

$$[K_{\hat{\theta}\hat{\theta}}]=\frac{2R_v-f(1-U_v)}{R\sqrt{2R_v-f}} \tag{49}$$

is easy while

$$[K_{\hat{n}\hat{n}}]=\frac{2R_{vv}(1-U_v)+2R_vU_{vv}+ff_r(1-U_v^3)}{2(2R_v-f)^{3/2}} -\frac{(f_v+3f_rR_v)(1+U_v^2)}{2(2R_v-f)^{3/2}} \tag{50}$$

is more complicated. In both of these calculations we have eliminated R_u using $R_u=\frac{R_v}{U_v}$ in the numerators and

$$\frac{1}{\sqrt{-f-2R_u}}=-\frac{U_v}{\sqrt{-f+2R_v}}, \tag{51}$$

which can be derived directly from (41), for denominators.

Now we specialize to the reflective and Ori matchings. For reflective $U_{vv}=0$ and so

$$S^{\text{ref}}_{\hat{n}\hat{n}}=\frac{R_v-f}{2\pi R\sqrt{2R_v-f}}, \tag{52}$$

$$S^{\text{ref}}_{\hat{\theta}\hat{\theta}}=\frac{R_v-f}{4\pi R\sqrt{2R_v-f}}+\frac{2R_{vv}+f_r(f-3f_rR_v)-f_v}{8\pi(2R_v-f)^{3/2}}, \tag{53}$$

while for Ori

$$U_{vv}=-\frac{2R_{vv}}{f}+\frac{2f_rR_v^2}{f^2}+\frac{2f_vR_v}{f^2} \tag{54}$$

and so

$$S^{\text{Ori}}_{\hat{n}\hat{n}}=0, \tag{55}$$

$$S^{\text{Ori}}_{\hat{\theta}\hat{\theta}}=\frac{f_v}{4\pi R\sqrt{2R_v-f}}. \tag{56}$$

Thus far B has been a general spacelike surface. However we are mainly interested in surfaces for which the matching is as smooth as possible and so now restrict our attention to B defined by

$$\mu=0\Leftrightarrow f_v=0. \tag{57}$$

Then by the discussion surrounding (7) the flow of energy in the ingoing null direction vanishes at B and can continuously switch from ingoing to outgoing.

That this physically motivated choice is achievable is demonstrated in Sec. IV, but for now we note that with $f_v=0$,

[2]Equivalent matchings have previously been discussed in [22–24] for matching spherically symmetric spacetimes along a surface of arbitrary signature.

$$S^{\rm Ori}_{\hat{i}\hat{j}} = 0, \tag{58}$$

while the reflective matching retains nonzero components.

In a little more detail for the polytropic fluid and a reflective matching:

$$f_v^{\rm p,r} = 0 \Leftrightarrow \left(\frac{\Xi}{r}\right)^{2k} = \frac{\Xi}{kr}\frac{1}{\frac{M_v}{\Xi_v}} \tag{59}$$

and we can apply the right-hand side equality to show that

$$f_r^{\rm p,r} = \frac{2M}{R^2}\left(1 - \frac{\Xi}{M}\frac{M_v}{\Xi_v}\right). \tag{60}$$

In particular note that if $\Xi(v) = \xi M(v)$ for some constant ξ, then f_r vanishes as well (but is still not sufficient to cause the reflective stress tensor to vanish). We will return to this in Sec. IV B.

C. Matching infalling and radiation solutions across B: Matter fields

We can also consider potential discontinuities in the matter fields across B, apart from the shell. We begin by considering jumps in the bulk stress-energy tensor.

1. Discontinuities in the bulk $T^{\rm bulk}_{ab}$

From the standard junction condition formalism, the stress-energy tensor for the full spacetime is

$$T_{ab} = \Theta^- T^-_{ab} + \delta_B S_{ab} + \Theta^+ T^+_{ab}, \tag{61}$$

where $\Theta^\pm = 1$ on $\mathcal{M}_\pm$ but vanishes on $\mathcal{M}_\mp$ and δ_B is a Dirac delta function centered on B. Thus even if there is no thin shell induced on B it is still possible to have a discontinuity in the bulk stress energy across B. The canonical example of such a jump is across the boundary separating the Friedmann-Robertson-Walker from the Schwarzschild region during Oppenheimer-Snyder collapse [25].

To see if there is such a discontinuity in our case we compare the limiting behavior of $T^{\rm bulk}_{ab}$ as we approach B from the $\mathcal{M}_-$ and $\mathcal{M}_+$ sides. These limits are easily calculated as the fields are continuous up to B. For $\mu = 0$ one can apply (4), (36), and (37) to find that at B:

$$T^{\rm bulk}_{ab} = \rho \hat{u}_a \hat{u}_b - \rho \hat{n}_a \hat{n}_b + P\tilde{q}_{ab}. \tag{62}$$

It is straightforward to see that $\rho^+ = \rho^-$ on B. From $f^+ = f^-$:

$$\frac{d}{d\lambda}(f^+(U(\lambda), R(\lambda))) = \frac{d}{d\lambda}(f^-(V(\lambda), R(\lambda))), \tag{63}$$

but since $f^-_u = f^+_v = 0$ (from $\mu = 0$) and $\dot{R} \neq 0$ this implies that

$$f^+_r = f^-_r \Leftrightarrow \rho^+ = \rho^-, \tag{64}$$

and the only possible stress-energy discontinuity is from the pressure:

$$\Delta T_{ab} = (P^+ - P^-)\tilde{q}_{ab}. \tag{65}$$

For the special case of a polytropic null fluid $P = k\rho$ and so there is no discontinuity in the stress-energy tensor.

The easiest way to do a $f^+ = f^-$ match for such a fluid is to require

$$M^-(V(\lambda)) = M^+(U(\lambda)) \quad \text{and} \quad \Xi^-(V(\lambda)) = \Xi^+(U(\lambda)). \tag{66}$$

This is also a physically convenient choice: for this matching when a shell bounces it will return to infinity with the same energy density M (and Ξ) as when it left.

2. Other discontinuities

It is possible to have discontinuities in fields that do not show up in either the boundary or bulk stress energy. For example, discontinuities in the electric field can signal the existence of thin shells of charge. This is a standard result from undergraduate electromagnetism but as an example in general relativity[3] consider two Reissner-Nordström spacetimes of the same mass but opposite charge attached across an $r =$ constant surface. The geometry is indifferent to the sign of the charge. In particular both the metric and stress energy depend only on the square of the charge:

$$f = 1 - \frac{2M}{r} + \frac{Q^2}{r^2}, \tag{67}$$

$$T_{ab} = \frac{Q^2}{8\pi r^4}(-q^\perp_{ab} + \tilde{q}_{ab}). \tag{68}$$

However in this case the stress-energy tensor is generated by the underlying Maxwell field:

$$F_{ab} = \frac{Q}{r^2}(\ell_a N_b - N_b \ell_a), \tag{69}$$

where ℓ and N are cross-normalized radial null vectors $\ell \cdot N = -1$ and $E_\perp = \frac{Q}{r^2}$ is the radial component of the electric field that can be integrated over surfaces of constant r to obtain the contained charge Q. Hence if $Q_{\rm in} = -Q_{\rm out}$, then even though there are no geometric or stress-energy discontinuities there is an induced (total) charge of $2Q_{\rm in}$ at the interface.

One could ask if similar discontinuities can arise in our more general models. The answer is no—unless there is an

[3]For further discussion of these matching conditions in spherically symmetric general relativity see, for example, [23,24].

underlying theory generating the μ, ρ, and P. Without an additional theory, all that there is the stress-energy tensor and so if that is continuous,[4] that is the end of the story. This is the situation for our general models except for the polytropic fluid with $k = 1$. There one can either (1) take μ, ρ, and P at face value as the energy densities and pressure associated with a null fluid or (2) reinterpret μ, ρ, and P as arising from charged null dust. From the perspective of the stress-energy tensor this distinction is irrelevant, however taking the Maxwell interpretation opens the possibility of an electric field discontinuity as discussed above.

Even with the null dust–Maxwell interpretation and thus VRN spacetimes there is no discontinuity for the (66) cases: if $Q^+ = Q^-$ and the metrics match then so do the normal components of the electric field. There is no thin shell of charge.

IV. BOUNCING NULL FLUID EXAMPLE

We have now seen several properties of the matching surface but have not yet established whether there is any $m(v, r)$ for which it exists with the properties that we have assumed. For example, is it actually possible to pick $m(v, r)$ so that $\mu = m_v = 0$ is spacelike and the surface is not inside a trapped region? In this section we demonstrate that at least one example exists.

A. Trapped and untrapped regions

First, we establish the location of the trapped regions in our spacetimes. For (27) the outward and inward null expansions are

$$\theta_{(\ell)} = \tilde{q}^{ab}\nabla_a \ell_b = \frac{\epsilon f}{r} \tag{70}$$

and

$$\theta_{(N)} = \tilde{q}^{ab}\nabla_a N_b = -\frac{2\epsilon}{r}. \tag{71}$$

Figure 1(a) shows spacetime with $\epsilon = 1$ and an infalling fluid. In that case spherical surfaces are outer trapped ($\theta_{(\ell)} < 0$) for $f < 0$, marginally outer trapped ($\theta_{(\ell)} = 0$) for $f = 0$ (that is, an apparent horizon), and outer untrapped ($\theta_{(\ell)} > 0$) for $f > 0$. For all of these $\theta_{(N)} < 0$ and so when $f < 0$ the surfaces are fully trapped and so inside a black hole.

By contrast Fig. 1(b) with $\epsilon = -1$ shows a radiating white hole spacetime. The apparent horizon is again at $f = 0$ but this time the shaded region is totally untrapped ($\theta_{(\ell)} > 0$, $\theta_{(N)} > 0$) when $f < 0$. So again the region of regular spacetime has $f > 0$.

[4]In fact it is not hard to see that polytropic fluids the components are actually C^1 and so overachieve this target. See Appendix C.

B. Linear matter

Thus the surface $\mu = 0$ is spacelike and always outside of the black and white hole regions if there is a choice of $M(v)$ and $\Xi(v)$ such that both

$$2\epsilon R_w - f(w, R(w)) > 0 \quad \text{and} \quad f(w, R(w)) > 0, \tag{72}$$

where $R(w)$ is implicitly defined by $f_w(w, R(w)) = 0$.

To see that these conditions can be met, consider the simple choice

$$\Xi(w) = \xi M(w), \tag{73}$$

where $\xi > 0$ is a constant. In the charged Vaidya case, ξ corresponds to the charge-to-mass ratio of the fluid. With this choice (20) gives that the junction hypersurface is

$$R(w) = \chi M(w), \tag{74}$$

where $\chi = \xi(k\xi)^{1/(2k-1)}$.

Then

$$\begin{aligned} f(w, R(w)) &= 1 - \frac{2}{\chi} + \left(\frac{\xi}{\chi}\right)^{2k} \\ &= 1 - \frac{1}{\chi}\left(\frac{2k-1}{k}\right) \end{aligned} \tag{75}$$

is constant along the surface and is positive (the shaded region of Fig. 2) if

$$\chi > \frac{2k-1}{k} \Leftrightarrow \xi > \frac{(2k-1)^{\frac{2k-1}{2k}}}{k}. \tag{76}$$

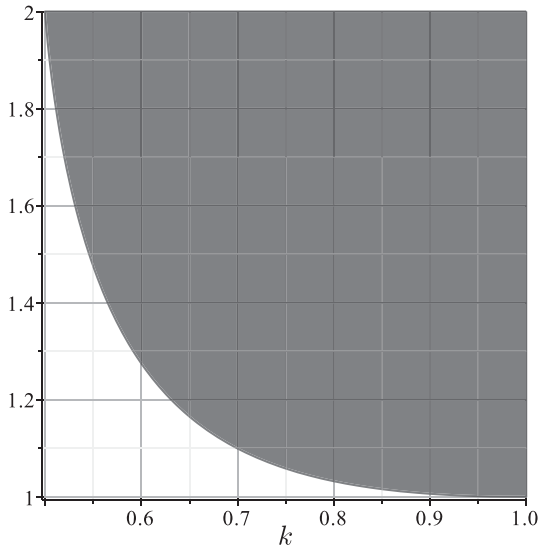

FIG. 2. Allowed values of ξ so that the surface $m_w = 0$ will be between the horizon and $r = \infty$.ξ must be chosen in the shaded region above $\frac{1}{k}(2k-1)^{\frac{2k-1}{2k}}$.

In particular note that for the $k = 1$ charged Vaidya case, this condition implies that the charge-to-mass ratio must be greater than 1. The special $(k = 1, \xi = 1)$ case is the dynamical extremal horizon considered in [10].

Next, the junction surface in the ingoing spacetime is spacelike if $2R_v \geq F$. That is, on applying (74),

$$M_v > \frac{f}{2\chi} = \frac{1}{2k\chi^2}(k\chi + 1 - 2k). \tag{77}$$

Thus for any choice of (k, ξ) there is a lower bound on M_v. Equivalently this is a lower bound on the allowed fluid energy at infinity (Appendix A). Because we have restricted our attention to junction surfaces outside the black hole this lower bound is necessarily positive: that is, there is a minimum allowed rate of expansion. Similarly in the radiating region there is a minimum allowed rate of contraction. This minimum is shown in Fig. 3.

In the extreme Vaidya limit $(k \to 1, \xi \to 1)$ this bound goes to zero but in all other cases it is positive. As such these constructed spacetimes can only describe continuous (eternal) expansions. They cannot describe spacetimes which either depart from or return to equilibrium. However once again it is important to emphasize that this is not a restriction on the allowed physics of spacetimes but rather a restriction on which spacetimes can be described by this particular model.

We now examine the stress energy at a reflective junction for this linear matter. Since both f_v and, by (60), f_r vanish the expressions become quite simple:

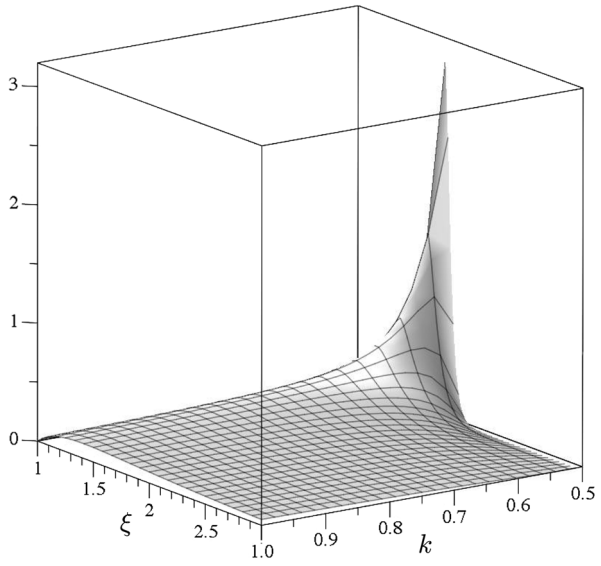

FIG. 3. Minimum values of M_v for infalling null fluids. M_v must be greater than the plotted surface for the junction surface to be spacelike. For the radiating side $-M_v$ must be greater than this value.

$$S^{\text{ref}}_{\hat{n}\hat{n}} = \frac{M_v - f/\chi}{2\pi\chi^{1/2}M\sqrt{2M_v - f/\chi}}, \tag{78}$$

where f is given by (75). Meanwhile from (53) we have

$$S^{\text{ref}}_{\hat{2}\hat{2}} = \frac{1}{4\pi\chi^{1/2}}\left(\frac{M_v - f/\chi}{M\sqrt{2M_v - f/\chi}} + \frac{M_{vv}}{(2M_v - f/\chi)^{3/2}}\right). \tag{79}$$

For the special case of linear accretion $M = (f/\chi)v$ both of these vanish, but in general that is not the case.

V. CONCLUSION

In this paper we have extended Ori's resolution of VRN energy condition violations to Husain null fluids. We saw that with his matching condition, the no-thin-shell bounce result extends to the Husain null fluids. The bounce is naturally caused by the fluid pressure.

By contrast for the reflective matching conditions used in [10], apart from a very special choice of the parameter functions, there continues to be a thin shell at the bounce surface. This is the physical cause of that bounce: it provides the necessary energy to turn the matter around. However note that it in itself can be interpreted as violating the energy conditions: it is pressure without a corresponding energy density.

We have also examined the bulk stress-energy tensor and have identified the conditions under which there are discontinuities in the bulk stress-energy tensor at B. For polytropic fluids with the most convenient matching conditions, the stress-energy tensor and its first derivatives are continuous across the transition. For the special case of VRN where the stress-energy tensor is interpreted as arising from a null dust–Maxwell system, there is no thin shell of charge on B.

Finally, we have explicitly demonstrated the existence of parameter choices $[\Xi(v) = \xi M(v)]$ such that the bounce surface is spacelike and outside of any trapped region. However we have also seen that these choices restrict us to describing cases where $M_v(v)$ is always greater than some positive constant. Thus it necessarily describes an eternally expanding junction surface. While this particular ansatz of solutions cannot describe departures from or returns to equilibrium it still serves to establish the existence of solutions for which our matching conditions apply.

ACKNOWLEDGMENTS

Thanks to John Bowden, Hari Kunduri, Viqar Husain, Matt Visser (in particular for his input on type II energy conditions), and Jessica Santiago for the useful discussions at various points during this work. Amos Ori helped us find a significant error in the first version of this paper. Substantial parts of the calculations were done while

I. B. was on sabbatical at Victoria University in Wellington, New Zealand, and he would like to thank the School of Mathematics and Statistics for their hospitality. I. B. and B. C. were both supported by NSERC Discovery Grant No. 261429-2013, while B. C. was also supported by a NSERC PGS-M Fellowship.

APPENDIX A: CHARGED NULL PARTICLE PATHS IN REISSNER-NORDSTÖM

A charged timelike particle moving in a spacetime with an electromagnetic field does not move along geodesics but instead with unit four-velocity $\hat{v}^a$ which obeys

$$\hat{v}^a \nabla_a \hat{v}^b = \frac{q}{m} F^b_c \hat{v}^c, \tag{A1}$$

where q and m are respectively its charge and mass. Similarly Ori [3] argued that the (null) "wave vector" k^a of a massless particle should obey

$$k^a \nabla_a k^b = q F^b_c k^c, \tag{A2}$$

where q is again the charge. The scaling of the null vector is significant as an observer with unit four-velocity u^a would measure it to have energy $E = -k \cdot u$. In particular we will find it useful to label these paths by their energy observed by an observer at infinity $E_\infty = -k \cdot u_\infty$.

We study the evolution of charged null particles in RN spacetime. We restrict our attention to particles moving radially and so while we already know that they must follow the same paths as null geodesics, (A2) will fix the scaling of the null vectors. We work with RN in ingoing Eddington-Finkelstein coordinates:

$$ds^2 = -f dv^2 + 2 dv dr + r^2 d\Omega^2, \tag{A3}$$

where $f = 1 - \frac{2M}{r} + \frac{Q^2}{r^2}$ in the usual way but unlike in the main text M and Q are constants. The associated electromagnetic field is generated by the potential

$$A = -\frac{Q}{r} dv \Rightarrow F = -\frac{Q}{r^2} dv \wedge dr. \tag{A4}$$

We work with a null dyad of the same form as in the main text:

$$\ell = \frac{\partial}{\partial v} + \frac{f}{2} \frac{\partial}{\partial r}, \tag{A5}$$

$$N = -\frac{\partial}{\partial r}. \tag{A6}$$

We consider ingoing and outgoing particles whose wave vectors necessarily take the form

$$k^- = g^-(r) N, \qquad k^+ = g^+(r) \ell \tag{A7}$$

for some functions $g^-(r)$ and $g^+(r)$ respectively. By (A2),

$$g^-(r) = E^-_\infty - \frac{qQ}{r}, \tag{A8}$$

$$g^+(r) = \frac{2}{f}\left(E^+_\infty - \frac{qQ}{r}\right). \tag{A9}$$

Thus the observer hovering at constant r with four-velocity

$$u = \frac{1}{\sqrt{f}} \frac{\partial}{\partial v} \tag{A10}$$

measures energies

$$E^- = \frac{1}{\sqrt{f}}\left(E^-_\infty - \frac{qQ}{r}\right), \tag{A11}$$

$$E^+ = \frac{1}{\sqrt{f}}\left(E^+_\infty - \frac{qQ}{r}\right), \tag{A12}$$

with E_∞ clearly being the limit as $r \to \infty$.

Then possible particle paths are shown in Fig. 4. Intuitively they can be understood as the electromagnetic field redshifting or blueshifting $k^\pm$ depending on whether or not the particle is moving with or against the field.[5] The energy vanishes at

$$r_o = \frac{qQ}{E^\pm_\infty}. \tag{A13}$$

That is, in order for the particle to have energy $E^\pm_\infty$ at infinity it must have zero energy at r_o. For particular choices of q, Q, and $E^\pm_\infty$ certain regions of spacetime are forbidden to (future-oriented) positive energy particles.

Ori then argued that physically it makes more sense to view particles reaching r_o as switching from ingoing to outgoing null paths rather than continuing in a straight line and thus becoming negative energy particles. Thus in Fig. 4 the ingoing particles in I_{++} redshift to zero energy at r_o and thus bounce to become the outgoing particles of O_{++}. Similarly the outgoing particles of O_{-+} bounce to become the ingoing particles of I_{-+}.

This same interpretation may be applied to the particles making up the charged fluid in Vaidya RN. In that case the particles making up the shell of constant v (or u) essentially move as if they were particles of charge

$$q = \frac{Q_v}{4\pi r^2} \tag{A14}$$

moving in a background RN spacetime with mass $M(v)$ and charge $Q(v)$.

[5]Thanks to Hari Kunduri for suggesting this interpretation.

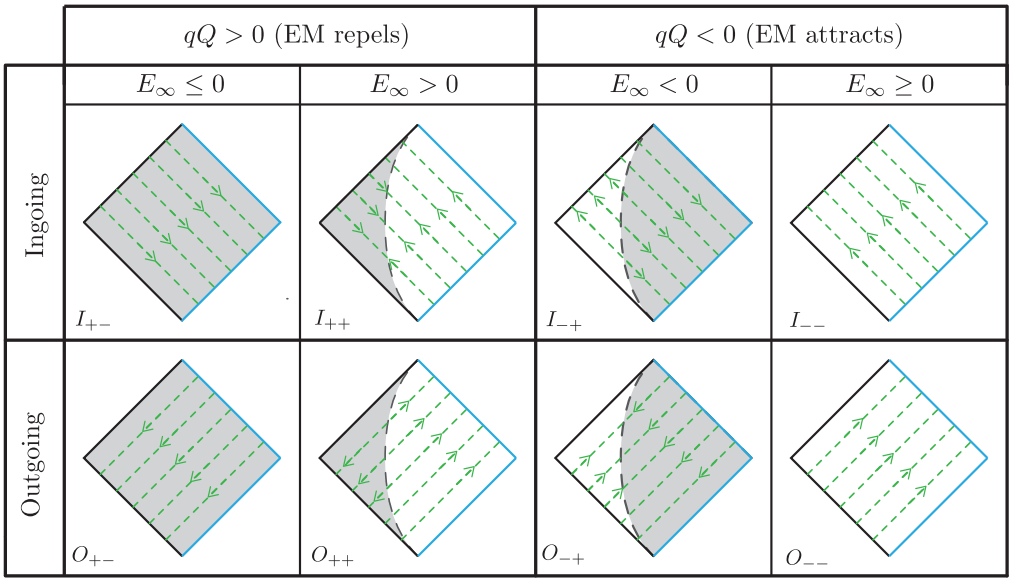

FIG. 4. Possible charged null particle paths in RN spacetimes. Only the region between the black and white hole event horizons and null is shown. The labels indicate whether the particle moves along ingoing (I) or outgoing (O) null paths with the first and second subscripts respectively indicating the signs of qQ and E_∞. Physically the gray forbidden zones can be best understood as resulting from an electromagnetic (EM) redshifting of the wave vector when the particle moves against the field or a blueshifting when the particle moves with the field. In the gray zones the energy becomes negative (or equivalently the particles must move backwards in time). The dividing line between zones is always located at $r = \frac{qQ}{E_\infty}$.

APPENDIX B: ENERGY CONDITIONS FOR TYPE II STRESS-ENERGY TENSORS

Stress-energy tensors are classified in [12] by their eigenvectors. For physical fields by far the most common are type I tensors which have a timelike eigenvector ξ^a whose eigenvalue is the (negative) energy density as measured by an observer with that four-velocity:

$$T^a{}_b\xi^b = -\mu\xi^a. \tag{B1}$$

However the focus of this paper is type II tensors which have no timelike eigenvector but instead have a double null eigenvector. Then for some tetrad $(\ell, N, e^{(2)}, e^{(3)})$ where ℓ and N are null, future oriented and cross scaled so that $\ell \cdot N = -1$ and $e^{(2)}$ and $e^{(3)}$ are orthonormal (to each other) and orthogonal to ℓ and N, the stress-energy tensor will necessarily take the form

$$T^{ab} = \mu N^a N^b - \rho q^{\perp ab} + P_2 e^a_{(2)} e^b_{(2)} + P_3 e^a_{(3)} e^b_{(3)}. \tag{B2}$$

Here $\mu \neq 0$ ($\mu = 0$ is type I) and $q^\perp_{ab}$ is as defined in (5). This particular arrangement of the constants has been chosen to be consistent with (4), though in that case note that $P_2 = P_3$.

Then we can consider the restrictions placed on μ, ρ, P_2, and P_3 by the energy conditions. The weak, dominant, and strong conditions are each based on measurements of the stress energy made by timelike observers. Thus we consider an arbitrary future-oriented unit timelike vector field which can be defined by parameters α, β, and γ:

$$\xi^a = \frac{\cosh\alpha}{\sqrt{2}}(e^\beta \ell^a + e^{-\beta} N^a) + \sinh\alpha((\cos\gamma)e^a_{(2)} + (\sin\gamma)e^a_{(3)}). \tag{B3}$$

The null energy condition is based on an arbitrary null vector which we write similarly as

$$k^a = \frac{e^\alpha}{\sqrt{2}}(e^\beta \ell^a + e^{-\beta} N^a) + e^\alpha((\cos\gamma)e^a_{(2)} + (\sin\gamma)e^a_{(3)}). \tag{B4}$$

It is then straightforward to check the energy conditions. We present these in more detail than the complexity of the calculations might warrant as the results differ from those presented in [12]. While the correct energy conditions have been noted and applied by others [13–16,26] it also true that the error in [12] does not seem to be universally known. The incorrect conditions are used in, for example, [2,9,17–21].

1. Weak energy condition

The weak energy condition $T_{ab}\xi^a\xi^b \geq 0$ says that no timelike observer sees negative energy densities. From (B2) and (B3) this becomes

$$\left(\frac{e^{2\beta}}{2}\mu+\rho\right)+(P_2\cos^2\gamma+P_3\sin^2\gamma)\tanh^2\alpha\geq 0 \quad \text{(B5)}$$

for all α,β,γ. By considering extreme cases we can find the bounds on μ, ρ, P_2, and P_3. Then

$$\alpha=0,\beta\to\infty\Rightarrow\mu\geq 0, \quad \text{(B6)}$$

$$\alpha=0,\beta\to-\infty\Rightarrow\rho\geq 0, \quad \text{(B7)}$$

while

$$\alpha\to\infty,\beta\to-\infty\Rightarrow\rho+P_i\geq 0$$

for $i\in\{2,3\}$. Other limits are redundant.

2. Null energy condition

The null energy condition replaces the timelike vector ξ^a in the weak energy condition with k^a. That is,

$$e^{2\beta}\mu+2\rho+2(P_2\cos^2\gamma+P_3\sin^2\gamma)\geq 0, \quad \text{(B8)}$$

where the e^α overall scaling of the null vector becomes irrelevant. Thus,

$$\beta\to\infty\Rightarrow\mu\geq 0, \quad \text{(B9)}$$

$$\beta\to-\infty\Rightarrow\rho+P_i\geq 0 \quad \text{(B10)}$$

for $i\in\{2,3\}$. Other limits are redundant and in the usual way this is implied by the weak energy condition.

3. Dominant energy condition

The dominant energy condition says that $-T^a_b\xi^a$ should be future directed and causal. That is, timelike observers should only see matter flowing forwards in time with speed less than or equal to the speed of light. Future-directed is ensured by

$$T_{ab}\xi^a\ell^b\geq 0\Rightarrow\mu e^{\beta}+\rho e^{-\beta}\geq 0\Rightarrow\mu,\rho\geq 0, \quad \text{(B11)}$$

with the corresponding N^a condition being redundant.

Causality implies that $\|T_{ab}\xi^b\|^2\leq 0$. This becomes

$$\rho(\mu e^{2\beta}+\rho)\cosh^2\alpha-(P_2^2\cos^2\gamma+P_3\sin^2\gamma)\sinh^2\alpha\geq 0. \quad \text{(B12)}$$

The $\alpha=0$ limit is redundant with (B11) however:

$$\alpha\to\infty,\beta\to-\infty\Rightarrow|P_i|\leq|\rho| \quad \text{(B13)}$$

for $i\in\{2,3\}$. Other limits are redundant.

4. Strong energy condition

The strong energy condition $R_{ab}\xi^a\xi^b\geq 0$ can be interpreted in a physical way but in essence is the geometric condition that must be assumed to prove results such as the singularity theorems. With our usual substitutions it becomes

$$0\leq\frac{1}{2}(e^{2\beta}\mu+P_2+P_3)+\left(\rho-\frac{1}{2}(1-2\cos^2\gamma)P_2-\frac{1}{2}(1-2\sin^2\gamma)P_3\right)\tanh^2\alpha. \quad \text{(B14)}$$

Then

$$\alpha=0,\beta\to\infty\Rightarrow\mu\geq 0, \quad \text{(B15)}$$

$$\alpha=0,\beta\to-\infty\Rightarrow P_2+P_3\geq 0, \quad \text{(B16)}$$

while

$$\alpha\to\infty,\beta\to-\infty\Rightarrow\rho+P_i\geq 0 \quad \text{(B17)}$$

for $i\in(2,3)$. Other limits are redundant.

5. Summary of energy conditions

To summarize, for a stress-energy tensor of form (B2) the energy conditions are

(1) Weak: $\mu\geq 0$, $\rho\geq 0$, $\rho+P_i\geq 0$
(2) Null: $\mu\geq 0$, $\rho+P_i\geq 0$
(3) Dominant: $\mu\geq 0$, $\rho\geq 0$, $|P_i|\leq|\rho|$
(4) Strong: $\mu\geq 0$, $P_2+P_3\geq 0$, $\rho+P_i\geq 0$.

If we restrict ourselves to type II stress-energy tensors of this form, then $\mu>0$.

As noted, individually these are not equivalent to the conditions given in [12]. However if $P_1=P_2$ and we require all of them to be satisfied simultaneously, then this is the same as requiring that all of the conditions in [12] be satisfied simultaneously. For anisotropic angular pressures ($P_1\neq P_2$) the combined conditions are not quite equivalent, as [12] also requires the pressures to be individually positive.

APPENDIX C: STRESS ENERGY IS C^1 ACROSS B

In this appendix we demonstrate that the stress energy of polytropic fluids is not only continuous across B, but the derivatives are also continuous. To see this we first derive the equations of motion governing the null fluid. Either by expanding the divergence of (4) or (equivalently) by combining (7)–(9) it is straightforward to show that they are

$$\mathcal{L}_N(\tilde{\varepsilon}\rho)+P\mathcal{L}_N\tilde{\varepsilon}=0, \quad \text{(C1)}$$

$$\mathcal{L}_\ell(\tilde{\varepsilon}\rho) + P\mathcal{L}_\ell\tilde{\varepsilon} = -\mathcal{L}_N(\tilde{\epsilon}\mu), \tag{C2}$$

where $\tilde{\varepsilon} = r^2 \sin^2\theta \mathrm{d}\theta \wedge \mathrm{d}\phi$ is the usual spherically symmetric area element. As always, these are conservation equations balancing evolving energy densities and work terms.

Now consider what these say about how the fields change across B. Writing the tangent and normal vectors as

$$X = \alpha\ell + \beta N, \tag{C3}$$

$$X_\perp = \alpha\ell - \beta N, \tag{C4}$$

the equations of motion (C1) and (C2) can be recast as

$$\begin{aligned}\mathcal{L}_X(\tilde{\varepsilon}\rho) + P\mathcal{L}_X\tilde{\varepsilon} &= \mathcal{L}_{X_\perp}(\tilde{\varepsilon}\rho) + P\mathcal{L}_{X_\perp}\tilde{\varepsilon} \\ &= \frac{\alpha}{2\beta}(\mathcal{L}_{X_\perp} - \mathcal{L}_X)(\tilde{\varepsilon}\mu).\end{aligned} \tag{C5}$$

On B with $f^+ = f^-$ and $\mu = 0$, we saw in Sec. III that intrinsic and extrinsic curvatures match and also $\rho^+ = \rho^-$. Then it immediately follows that

$$\begin{aligned}(\Delta P)\mathcal{L}_X\tilde{\varepsilon} &= \tilde{\varepsilon}(\Delta\mathcal{L}_{X_\perp}\rho) + (\Delta P)\mathcal{L}_{X_\perp}\tilde{\varepsilon} \\ &= \tilde{\varepsilon}\frac{\alpha}{2\beta}\Delta(\mathcal{L}_{X_\perp}\mu),\end{aligned} \tag{C6}$$

where $\Delta P = P^+ - P^-$ and similarly for the other quantities. Hence discontinuities in P imply discontinuities in the normal derivatives of μ and ρ. However for polytropic models $P = k\rho$ and thus not only do μ, ρ, and P match across B but so do their normal derivatives.

By the matching conditions we already know that the tangential derivatives are continuous. Hence the derivatives of the stress-energy components are also continuous.

[1] W. B. Bonnor and P. C. Vaidya, Spherically symmetric radiation of charge in Einstein-Maxwell theory, Gen. Relativ. Gravit. **1**, 127 (1970).
[2] V. Husain, Exact solutions for null fluid collapse, Phys. Rev. D **53**, R1759 (1996).
[3] A. Ori, Charged null fluid and the weak energy condition, Classical Quantum Gravity **8**, 1559 (1991).
[4] K. Lake and T. Zannias, Structure of singularities in the spherical gravitational collapse of a charged null fluid, Phys. Rev. D **43**, 1798 (1991).
[5] Y. Kaminaga, A dynamical model of an evaporating charged black hole and quantum instability of Cauchy horizons, Classical Quantum Gravity **7**, 1135 (1990).
[6] A. Ashtekar and B. Krishnan, Isolated and dynamical horizons and their applications, Living Rev. Relativ. **7**, 10 (2004).
[7] I. Booth, Black hole boundaries, Can. J. Phys. **83**, 1073 (2005).
[8] T. Dray, Bouncing shells, Classical Quantum Gravity **7**, L131 (1990).
[9] S. Chatterjee, S. Ganguli, and A. Virmani, Charged Vaidya solution satisfies weak energy condition, Gen. Relativ. Gravit. **48**, 91 (2016).
[10] I. Booth, Evolutions from extremality, Phys. Rev. D **93**, 084005 (2016).
[11] W. Israel, Singular hypersurfaces and thin shells in general relativity, Nuovo Cimento B **44**, 1 (1966).
[12] S. W. Hawking and G. F. R. Ellis, *The Large Scale Structure of Space-Time*, Cambridge Monographs on Mathematical Physics (Cambridge University Press, Cambridge, England, 2011).
[13] M. Mars, M. Mercè Martín-Prats, and J. M. M. Senovilla, Models of regular Schwarzschild black holes satisfying weak energy conditions, Classical Quantum Gravity **13**, L51 (1996).
[14] A. Levy and A. Ori (private communication).
[15] P. Martín-Moruno and M. Visser, Classical and quantum flux energy conditions for quantum vacuum states, Phys. Rev. D **88**, 061701 (2013).
[16] Anonymous referee (private communication).
[17] A. Wang and Y. Wu, Generalized Vaidya solutions, Gen. Relativ. Gravit. **31**, 107 (1999).
[18] T. Harko and K. S. Cheng, Collapsing strange quark matter in Vaidya geometry, Phys. Lett. A **266**, 249 (2000).
[19] S. G. Ghosh and N. Dadhich, Gravitational collapse of type II fluid in higher dimensional space-times, Phys. Rev. D **65**, 127502 (2002).
[20] U. Debnath, N. C. Chakraborty, and S. Chakraborty, Gravitational collapse in higher dimensional Husain space-time, Gen. Relativ. Gravit. **40**, 749 (2008).
[21] S. G. Ghosh and D. Kothawala, Radiating black hole solutions in arbitrary dimensions, Gen. Relativ. Gravit. **40**, 9 (2008).
[22] M. Merce Martin-Prats, Ph. D. thesis, University of Barcelona, 1995.
[23] F. Fayos, J. M. M. Senovilla, and R. Torres, General matching of two spherically symmetric space-times, Phys. Rev. D **54**, 4862 (1996).
[24] F. Fayos, J. M. M. Senovilla, and R. Torres, Spherically symmetric models for charged radiating stars and voids: I. Charge bound, Classical Quantum Gravity **20**, 2579 (2003).
[25] J. R. Oppenheimer and H. Snyder, On continued gravitational contraction, Phys. Rev. **56**, 455 (1939).
[26] P. Martin-Moruno and M. Visser, Classical and semiclassical energy conditions, Fundam. Theor. Phys. **189**, 193 (2017).